

Multiperipheral model of direct muon production*

Gilbert Chu

Lawrence Berkeley Laboratory, University of California, Berkeley, California 94720

Joel Koplik

Department of Physics, Columbia University, New York, New York 10027

(Received 3 March 1975)

We discuss the production of massive $\mu\bar{\mu}$ pairs in pp collisions at high energy using the pion-exchange multiperipheral model. The reaction is assumed to proceed through the sequence (virtual $\pi^+\pi^-$) $\rightarrow \gamma \rightarrow \mu\bar{\mu}$, with a pion form factor included at the first stage. We present both numerical results for various cross sections of interest and some general results following from a Regge expansion. In particular, we find a scaling law for $d\sigma/dq^2$ easily distinguishable from the parton-model analog. The numerical results are in rough agreement with presently available data, and we conclude that the bulk of muon-pair production can be attributed to familiar hadronic mechanisms.

1. INTRODUCTION

An understanding of the production of lepton pairs in hadronic collisions must be an important facet in the study of photon-hadron interactions. It has been shown that the parton model leads to specific predictions for the cross sections in terms of deep-inelastic scattering.¹⁻³ However, recent analyses have indicated a serious discrepancy between the model⁴⁻⁷ and the data.^{8,9} One's thoughts then turn naturally to alternative explanations, particularly those involving familiar strong-interaction concepts, and in this paper we use the pion-exchange multiperipheral model¹⁰ to study μ -pair production.¹¹

Explicitly, our model is the following: We assume that μ pairs occur as the decay products of a massive virtual photon which can appear along with the usual systems of hadrons that are produced in a multiperipheral chain. The amplitude is depicted in Fig. 1, and if we square, integrate over the phase space of the other hadrons, and sum over all possible produced particles besides the μ pair, we obtain the inclusive cross section of Fig. 2. The ingredients which enter into the

calculation of the μ -pair cross section are then the off-shell πp absorptive parts, the pion propagator, and the pion electromagnetic form factor.

This model was first studied by Subbarao¹²; however, he did not attempt to compare the results to experiment. Some numerical calculations, using a different method but essentially the same physical assumptions as the present calculation, have been given by Thacker,¹³ but we disagree with some of the details of this reference.

There are several inherent approximations involved in our procedure. First, it is known that a multiperipheral model based on pion exchange alone is unrealistic in that the low-energy $\pi\pi$ cross sections (which are iterated to build the high-energy cross section) are too small, and the resulting Regge poles are much too low.¹⁴ Second, some form for the off-shell extrapolation of the πp absorptive parts and the $\pi\pi\gamma$ vertex must be chosen. We deal with both difficulties by constructing an analogous model for pion production via ρ -meson decay. That is, we replace the $\pi\pi\gamma \rightarrow \mu\bar{\mu}$ vertices in Fig. 2 by the corresponding quantities for $\pi\pi \rightarrow \rho \rightarrow \pi\pi$, shown in Fig. 3, and adjust the over-all normalization and off-shell

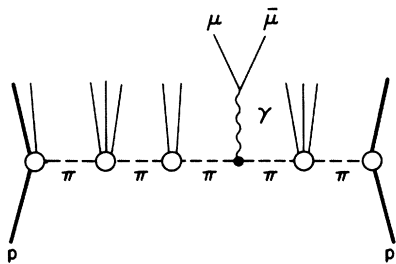


FIG. 1. Multiperipheral model of the μ -pair amplitude.

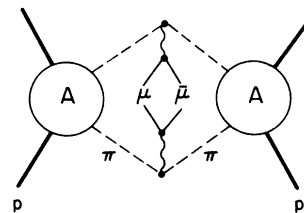


FIG. 2. The μ -pair inclusive cross section. The blobs labeled A denote off-shell π - p absorptive parts.

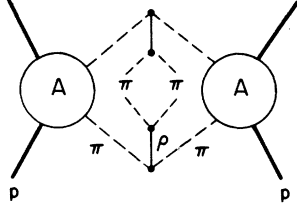


FIG. 3. Model for the pion inclusive cross section via ρ decay.

dependence to agree with the pion transverse momentum distribution at $E_{\text{lab}} = 300$ GeV. Then, with the same normalization and off-shell dependence, we compute the μ -pair cross section. This in effect assumes that high-energy hadronic cross sections are built from multiperipheral "pionlike" processes and, in this way, the successful predictions of multiperipheral models are retained.

An additional source of uncertainty is that the pion form factor is not known for large values of q^2 (photon mass squared) and we will assume the standard asymptotic behavior: $F_\pi(q^2) \sim 1/q^2$. Lastly, we will be neglecting photon emission from virtual nucleon (or baryon) lines, as in Fig. 4, mainly because nothing is known about the form factors of off-shell nucleons. As noted by Subbarao,¹² this process could be an important ingredient of the μ -pair cross section at lower energies and in the fragmentation regions of the incident particles. One hopes that the couplings of far-off-shell nucleons are suppressed, and in any case the fact that the form factor of the nucleon falls faster with q^2 than that of the pion will reduce its contribution. In view of these approximations one could not expect the result of the calculation to be very accurate, but it should be correct at least in order of magnitude, and the model is such an obvious candidate that it deserves a test.

Recent experiments¹⁵ have established the existence of new, massive particles which couple to the μ -pair channel. This phenomenon has not been included in the present calculation largely because

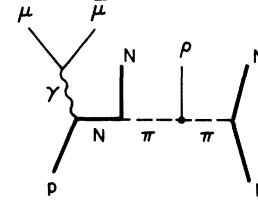


FIG. 4. μ -pair emission from a virtual nucleon (neglected in this paper).

the actual cross section for the new particles is small, so their effect can be omitted without damage to the main intent of this paper. In any case the large masses of the new particles ($\sim 3-4$ GeV) correspond to values of Q^2 where the physical basis of the model is uncertain and the pion form factor is not well known.

In Sec. II we discuss kinematics and the specific parametrizations used, and derive formulas for assorted μ -pair cross sections. Section III presents the Mueller-Regge expansions appropriate to the problem, and derives, using a rather general argument, the scaling law

$$\frac{d\sigma}{dq^2} = \frac{1}{q^4} [F_\pi(q^2)]^2 G(s/q^2).$$

This differs from the parton-model result by the factor F_π^2 . In Sec. IV we compare the model to existing data and present its predictions for other experiments. For reasons discussed below, the theoretical results are obtained by numerical integration rather than via the Regge expansion.

The results of the calculation are in rather good agreement with experiment for low and moderate values of photon mass and transverse momentum, where the model is most reliable and where most of the direct muon production occurs. In view of the approximations made the detailed numerical agreement is perhaps fortuitous, but we believe we have shown that the bulk of muon-pair production in pp collisions can be understood in terms of familiar hadronic processes.

II. KINEMATICS

We begin the analysis by deriving expressions for μ -pair cross sections suitable for numerical integration. Consider a typical μ -pair event in which $n+m$ additional particles are produced, and with momenta labeled as in Fig. 5. The corresponding cross section is

$$\lambda^{1/2}(s, m_p^2, m_p^2) d\sigma_{n+m+\mu\bar{\mu}} = \frac{1}{2} (2\pi)^4 \delta^4(p_1 + p_2 - p_+ - p_- - \sum k_i - \sum k'_i) \prod dk_i \prod dk'_i |T_{n+m+\mu\bar{\mu}}|^2, \quad (1)$$

where we use the abbreviations

$$\lambda(x, y, z) \equiv x^2 + y^2 + z^2 - 2(xy + yz + zx)$$

and

$$dk \equiv d^3k / [(2\pi)^3 2E] . \quad (2)$$

By assumption, the amplitude T takes the form

$$T_{\pi^+ m + \mu \bar{\mu}} = T_{\pi p \rightarrow n}(p_1, Q_1, k_1) \frac{1}{Q_1^2 - m_\pi^2} \left[\frac{e^2}{Q^2} \Gamma_\mu(Q_1, Q_2) \bar{u}(p_-) \gamma^\mu v(p_+) \right] \frac{1}{Q_2^2 - m_\pi^2} T_{\pi p \rightarrow m}(p_2, Q_2, k_1') , \quad (3)$$

where the momenta Q_i are shown in Fig. 5 and Γ_μ is the $\pi\pi\gamma$ vertex function

$$\Gamma_\mu(Q_1, Q_2) = (Q_1 - Q_2)_\mu F_\pi(Q^2) . \quad (4)$$

We insert Eq. (3) into Eq. (1) and sum over n and m ; this gives the inclusive μ -pair cross section as

$$\begin{aligned} \lambda^{1/2}(s, m_p^2, m_p^2) d\sigma &= \frac{2}{(2\pi)^4} \delta^4(Q + Q_1 + Q_2) d^4Q d^4Q_1 d^4Q_2 \\ &\times A_{\pi p}(p_1, Q_1) \frac{1}{(Q_1^2 - m_\pi^2)^2} L(Q, Q_1, Q_2) \frac{1}{(Q_2^2 - m_\pi^2)^2} A_{\pi p}(p_2, Q_2) , \end{aligned} \quad (5)$$

where we have introduced the (off-shell) πp absorptive part

$$A_{\pi p}(p_1, Q_1) = \sum_n \int \frac{1}{2} (2\pi)^4 \delta^4\left(p_1 + Q_1 - \sum_1^n k_i\right) \prod_1^n dk_i |T_{\pi p \rightarrow n}|^2 \quad (6)$$

and the lepton kernel

$$L(Q, Q_1, Q_2) = \frac{e^4}{Q^4} \Gamma_\lambda(Q_1, Q_2) \Gamma_\nu(Q_1, Q_2) \int dp_+ dp_- \delta^4(p_+ + p_- - Q) \text{Tr}[(\not{p}_- + m_\mu) \gamma^\lambda (\not{p}_+ - m_\mu) \gamma^\nu] . \quad (7)$$

Performing the trace and integration in Eq. (7) and neglecting terms of order m_μ^2/Q^2 ,

$$L(Q_1, Q_2) \approx L(Q^2, Q_1^2, Q_2^2) = \frac{e^4}{3(2\pi)^5} [F_\pi(Q^2)]^2 \frac{\lambda(Q^2, Q_1^2, Q_2^2)}{Q^4} . \quad (8)$$

If we introduce into Eq. (5) the quantity

$$1 = \int d^4K_1 d^4K_2 ds_1 ds_2 \delta^4(K_1 + p_1 - Q_1) \delta^4(K_2 + p_2 - Q_2) \delta(K_1^2 - s_1) \delta(K_2^2 - s_2)$$

and integrate over Q_1 and Q_2 , we find

$$\begin{aligned} \lambda^{1/2}(s, m_p^2, m_p^2) d\sigma &= Z \frac{2}{(2\pi)^4} \int ds_1 ds_2 \left\{ d^4Q d^4K_1 d^4K_2 \delta(K_1^2 - s_1) \delta(K_2^2 - s_2) \delta^4(p_1 + p_2 - K_1 - K_2 - Q) \right. \\ &\quad \left. \times A_{\pi p}(p_1, K_1 - p_1) \frac{1}{(t_1 - m_\pi^2)^2} L(Q^2, t_1, t_2) \frac{1}{(t_2 - m_\pi^2)^2} A_{\pi p}(p_2, K_2 - p_2) \right\} , \end{aligned} \quad (9)$$

where $t_{1,2} \equiv (p_{1,2} - K_{1,2})^2$. We have at this point inserted a normalization constant Z which, as described in the Introduction, will be chosen to agree with pion inclusive data. Note that Eq. (9) is really a sum of two terms involving either $A_{\pi^+ p}(p_1, K_1 - p_1) A_{\pi^- p}(p_2, K_2 - p_2)$ or $A_{\pi^- p}(p_1, K_1 - p_1) A_{\pi^+ p}(p_2, K_2 - p_2)$. The advantage of this expression is that it takes the form of an integral over s_1 and s_2 of a quasi-three-body phase-space integral, for which there exist standard numerical integration routines.

As discussed in the Introduction, we will fix the normalization by computing the transverse momentum distribution of pions, as produced by ρ decay. This is accomplished by replacing the lepton kernel $L(Q, Q_1, Q_2)$ by a corresponding ρ kernel

$$R(Q, Q_1, Q_2) = \int dp_a dp_b \delta^4(p_a + p_b - Q) |A_{\pi\pi}|^2 , \quad (10)$$

where p_a and p_b are the momenta of the produced pions and

$$A_{\pi\pi} = \frac{48\pi\Gamma_\rho m_\rho^2}{(m_\rho^2 - 4m_\pi^2)^{3/2}} (Q_1 - Q_2) \cdot (p_a - p_b) \frac{1}{s - m_\rho^2 + i\Gamma_\rho m_\rho} \quad (11)$$

When comparing the model to extant Fermilab data,⁹ which are in the form of a single- μ cross section, a modified formula is required. If in the preceding development we isolate the μ^+ phase-space element while integrating over the μ^- momentum we find

$$\begin{aligned} \lambda^{1/2}(s, m_\rho^2, m_\rho^2) \frac{d\sigma}{dp_+} &= \frac{4\alpha^2}{(2\pi)^5} \frac{1}{Q^4} [F_\pi(Q^2)]^2 \\ &\times \int A_{\pi\rho}(p_1, K_1 - p_1) \frac{1}{(t_1 - m_\pi^2)^2} \frac{1}{(t_2 - m_\pi^2)^2} A_{\pi\rho}(p_2, K_2 - p_2) \\ &\times [2(Q_1 - Q_2) \cdot p_-(Q_1 - Q_2) \cdot p_+ - (Q_1 - Q_2)^2 \frac{1}{2} Q^2] \\ &\times \delta^4(p_- + K_1 + K_2 - p_1 - p_2 + p_+) ds_1 ds_2 d^4 K_1 d^4 K_2 \delta(K_1^2 - s_1) \delta(K_2^2 - s_2) d^4 p_- \delta(p_-^2 - m_\mu^2). \end{aligned} \quad (12)$$

This is again an integration over 3-body phase space, which is performed numerically.

Finally, we describe the off-shell extrapolation used. Our choice is (loosely) motivated by the behavior of the multiperipheral model itself. It is known¹⁰ that if the low-energy multiperipheral kernel is assumed to have no off-shell dependence, then in a limit where first the energy (s) becomes large and then an external mass (u) becomes large and spacelike, but with $s \gg |u|$, an off-shell forward absorptive part $A(s; u)$ has the behavior

$$A(s; u) \rightarrow s^\alpha \left(\frac{|u|}{m^2} \right)^{-\alpha-1}, \quad (13)$$

where α is the leading Regge pole and m is the produced mass associated with the kernel. In the present situation, the kinematic requirements for Eq. (13) are not always met, the subenergies in $A_{\pi\rho}$ are usually not large enough for a single-term Regge expansion to suffice, and a range of values for m is called for. Furthermore, there is no reason for the kernel itself to have no off-shell dependence. We then allow some latitude by writing

$$A_{\pi\rho}(p, Q) = \sum_i r_i \left(\frac{p \cdot Q}{s_0} \right)^{\alpha_i} \left(\frac{m^2 - m_\pi^2}{m^2 - Q^2} \right)^{\alpha_i + n}, \quad (14)$$

where $s_0 = 1 \text{ GeV}^2$, r_i and α_i are chosen to fit the on-shell absorptive part, and we experiment with different values of m^2 and n to reproduce the observed pion transverse momentum distribution. The normalization factor Z in Eq. (9) will depend on the particular off-shell extrapolation chosen and should properly be written $Z(n, m)$.

III. THE SCALING LAW AND REGGE EXPANSION

A multiperipheral model naturally leads to a Regge expansion of an inclusive cross section and

in the present case, to a scaling law for $d\sigma/dq^2$. While we will not make direct use of these in comparing the model with data, the Regge expansion may be useful in the analysis of future experiments, and the scaling law provides an interesting contrast to the parton-model result.¹⁻³

The essential ingredient used in this section is the $O(3, 1)$ symmetry and corresponding partial diagonalization of the pion-exchange model. We define a partial-wave amplitude as¹⁶

$$A(\lambda; u, v) = \int_{s_0}^{\infty} ds e^{-(\lambda+1)\theta(s, u, v)} A(s; u, v), \quad (15)$$

where $A(s; u, v)$ is a forward two-body absorptive part with external squared masses u and v , and

$$\cosh\theta(s, u, v) = \frac{s - u - v}{2(uv)^{1/2}}. \quad (16)$$

$A(\lambda; u, v)$, as well as forward n -body amplitudes, can be expressed in terms of the $\pi\pi$ partial-wave amplitude as the solution of an integral equation with respect to momentum transfer. In particular, the contribution of μ -pair production to $A(\lambda; u, v)$ enters only through the transform (15) of its contribution to the $\pi\pi$ forward absorptive part, i.e.,

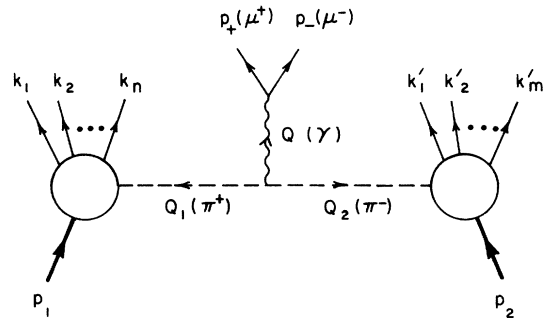


FIG. 5. Kinematics of the μ -pair amplitude.

through the factor

$$L(\lambda; u, v) = \int_0^\infty dQ^2 e^{-(\lambda+1)\theta(Q^2, u, v)} L(Q^2, u, v), \quad (17)$$

where $L(Q^2, u, v)$ was defined in Eqs. (7) and (8) above. We assume the peripherality of pion exchanges, so that typical momentum transfers entering into the multiperipheral chain are bounded, and thus for sufficiently large Q^2

$$\cosh\theta(Q^2, u, v) \approx \frac{1}{2} e^{\theta(Q^2, u, v)} \approx \frac{Q^2}{2(uv)^{1/2}}.$$

The numerical results described below indicate that this approximation is reasonably accurate for $Q^2 \gtrsim 3 \text{ GeV}^2$. This means

$$L(\lambda; u, v) \approx c(uv)^{(\lambda+1)/2} \int_0^\infty dQ^2 [F_\pi(Q^2)]^2 (Q^2)^{-\lambda-1}, \quad (18)$$

where c is a numerical constant.

It is convenient to extract particular values of Q^2 from the partial-wave projected equations by the device of functional differentiation with respect to the pion form factor. We shall later need the result

$$\frac{\delta L(\lambda; u, v)}{\delta F_\pi(q^2)} \propto F_\pi(q^2) (q^2)^{-\lambda-1}, \quad (19)$$

where the proportionality is up to factors independent of q^2 .

We first consider the scaling law. The idea of the derivation is that $d\sigma/dq^2$ is essentially an average multiplicity, and can be computed by differentiating the total cross section with respect to the "coupling constant."¹⁰ From Eq. (5) it is easy to show that

$$\begin{aligned} \frac{d\sigma}{dq^2} = & \lambda^{-1/2} (s, m_p^2, m_p^2) \frac{2}{(2\pi)^4} \int d^4Q_1 d^4Q_2 \delta^4(Q + Q_1 + Q_2) A_{\pi p}(p_1, Q_1) \frac{1}{(Q_1^2 - m_\pi^2)^2} \\ & \times d^4Q \delta(Q^2 - q^2) L(Q^2, Q_1^2, Q_2^2) \frac{1}{(Q_2^2 - m_\pi^2)^2} A_{\pi p}(p_2, Q_2). \end{aligned} \quad (20)$$

We can express this in terms of the total cross section as

$$\frac{d\sigma}{dq^2} = \frac{1}{2} F_\pi(q^2) \frac{\delta\sigma_{\text{tot}}}{\delta F_\pi(q^2)}. \quad (21)$$

The total cross section, in turn, is related to the partial-wave amplitude through the inverse transform of Eq. (15):

$$\sigma_{\text{tot}} = \frac{1}{\lambda^{1/2} (s, m_p^2, m_p^2)} \int_{c-i\infty}^{c+i\infty} \frac{d\lambda}{2\pi i} \frac{e^{(\lambda+1)\theta(s, m_p^2, m_p^2)}}{2m_p^2 \sinh\theta(s, m_p^2, m_p^2)} A(\lambda; m_p^2, m_p^2), \quad (22)$$

where $\text{Re}(c)$ is to the right of the singularities of A . Now the only dependence on the pion form factor occurs through the functional dependence of A on $L(\lambda; u, v)$. Thus, from Eq. (19),

$$\begin{aligned} \frac{\delta A(\lambda; m_p^2, m_p^2)}{\delta F_\pi(q^2)} &= \int du dv \frac{\delta A(\lambda; m_p^2, m_p^2)}{\delta L(\lambda; u, v)} \frac{\delta L(\lambda; u, v)}{\delta F_\pi(q^2)} \\ &= F_\pi(q^2) (q^2)^{-\lambda-1} g_1(\lambda). \end{aligned} \quad (23)$$

If we combine Eqs. (21)–(23), and assume $s \gg m_p^2$, we have

$$\frac{d\sigma}{dq^2} = \frac{1}{q^4} [F_\pi(q^2)]^2 \int_{c-i\infty}^{c+i\infty} \frac{d\lambda}{2\pi i} \left(\frac{s}{q^2}\right)^{\lambda-1} g_2(\lambda). \quad (24)$$

Here g_1 and g_2 are functions of λ but not of s or q^2 , so

$$\frac{d\sigma}{dq^2} = \frac{1}{q^4} [F_\pi(q^2)]^2 G(s/q^2). \quad (25)$$

In a model involving Regge poles alone we can be more explicit. Because of the differentiation in Eq. (23), $g_i(\lambda)$ will contain dipoles as well as poles in λ , which leads to

$$G(s/q^2) = \sum_\alpha \left(\frac{s}{q^2}\right)^{\alpha-1} \left(\gamma_\alpha \ln \frac{s}{q^2} + \gamma'_\alpha\right). \quad (26)$$

A special case of this result was first derived by Subbarao.¹²

A multiperipheral model of course gives a Regge expansion for the inclusive (differential) virtual-photon cross section. This is not overly useful at present (low) energies and for very massive photons because nonleading singularities are likely to dominate, but if μ -pair experiments are performed at higher energies a Regge expansion may provide a useful parametrization. Except for the Q^2 dependence of the photon coupling, which enters through Eq. (17), this problem has been treated

before^{17, 18} and we merely state the results.

For a virtual photon in the fragmentation region we have in the limit $s \rightarrow \infty$, $s/Q^2 \rightarrow \infty$

$$\frac{d\sigma}{d^4Q} \sim \frac{1}{Q^4} [F_\pi(Q^2)]^2 \sum_\alpha \left(\frac{s}{Q^2}\right)^{\alpha-1} r_\alpha \left(\frac{Q_{\parallel}^2}{Q^2}, \frac{Q_{\perp}^2}{Q^2}\right), \quad (27)$$

where $\alpha \equiv \alpha(0)$ is a trajectory intercept and r_α a (factorized) residue function, with Q_{\parallel} and Q_{\perp} measured in the rest frame of the fragmenting particle. Similarly, for the pionization region in the limit $s_1 = (p_1 + Q)^2 \rightarrow \infty$, $s_2 = (p_2 + Q)^2 \rightarrow \infty$, and $s_4/Q^2 \rightarrow \infty$, we find

$$\frac{d\sigma}{d^4Q} \sim \frac{1}{Q^2 s} [F_\pi(Q^2)]^2 \times \sum_{\alpha_1, \alpha_2} \left(\frac{s_1}{Q^2}\right)^{\alpha_1} \left(\frac{s_2}{Q^2}\right)^{\alpha_2} r_{12} \left(\frac{Q_{\perp}^2}{Q^2}\right). \quad (28)$$

Given a specific multiperipheral model one can explicitly determine the poles and residue functions r_α and r_{12} , but the latter turns out to take the form of an infinite sum which converges slowly, and is therefore not useful for numerical calculation.

IV. COMPARISON WITH EXPERIMENT

The existing data on μ -pair production in pp collisions consist of detailed distributions with respect to virtual photon mass and momentum at Brookhaven⁸ and single-muon cross sections at Fermilab.⁹ More detailed results both at Fermilab and at the CERN ISR are expected soon. We will compare the model to the Brookhaven and Fermilab experiments separately, and also make predictions for the other experiments.

First, we describe the parametrization of the amplitude and the off-shell extrapolation. For on-shell πp absorptive parts [see Eq. (14)] we assume $\alpha_1 = 1$ and $r_1 = 22.5 \text{ mb GeV}^2$, corresponding to asymptotically constant $\pi^+ p$ cross sections of 22.5 mb. The low-energy part is interpolated smoothly for $\pi^+ p$ by $r_2 = 50.5 \text{ mb GeV}^2$ and $\alpha_2 = -0.06$, and for $\pi^- p$ by $r_2 = 29.9 \text{ mb GeV}^2$ and $\alpha_2 = 0.33$.¹⁹ A possible asymptotic increase in πp cross sections would have a negligible effect on the results. The parameters m and n in Eq. (14) are found by requiring the model to yield the shape of pion transverse momentum distributions observed at Fermilab,²⁰ and a convenient choice is $n = 2$ and $m = 1 \text{ GeV}$. The normalization of the pion inclusive data is then obtained by choosing the normalization constant $Z = 90$ [see Eq. (9)]. The fit is shown in Fig. 6, where the ρ^0 distribution has been included for reference. The damping in the ρ^0 distribution is significantly

weaker than in the π^+ damping for kinematical reasons: The decay pions must share the ρ momentum and have the angular distribution appropriate to a $J = 1$ resonance.²¹

The value of Z depends very strongly on the choice of off-shell extrapolation; for example, for the choices $n = 1$ and $m^2 = 3 \text{ GeV}^2$ we would have $Z = 5$. Similar results on the normalization of cross sections in a pion-exchange multiperipheral model have been found by Tan and Tow.²² They conclude that a literal pion-exchange model is necessarily unrealistic. We, instead, take the point of view that for the purpose of our calculation the choice of Z is a phenomenological way of including the effect of all possible exchanges leading to pion production. The reason we discuss pion exchange at all is to estimate the coupling of virtual photons to the exchanged hadronic systems. The assertion of this paper is that a multiperipheral model which accounts for hadronic multiparticle production accounts for most direct leptons as well.

Note that we have fixed the parameters of the model by reproducing the pion transverse momentum distribution for p_{\perp} between 1 and 8 GeV/c, and have thereby asserted that all such pions originate from ρ meson decay. The experimental situ-

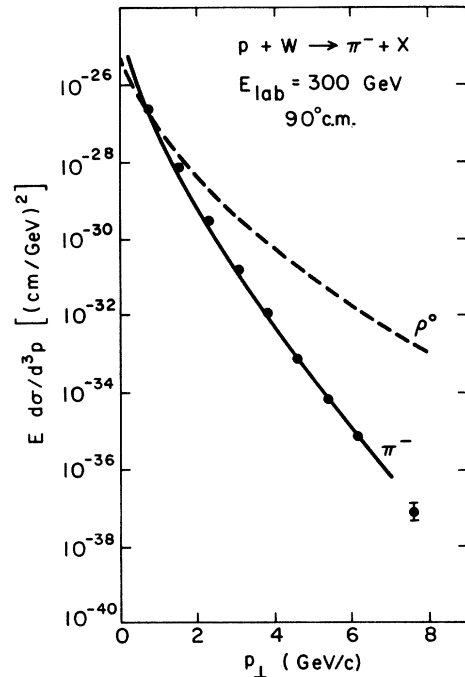


FIG. 6. Pion transverse momentum distribution. The data are from Ref. 20. The curves indicate the fitted pion distribution (solid) and the corresponding ρ distribution (dashed).

ation is not completely clear on this point, but the Brookhaven data of Gordon *et al.*²³ do exhibit the crossover at $p_{\perp} \approx 1$ GeV/c predicted in Fig. 6. The same data also indicate that the ρ transverse momentum distribution is much broader than that of the pion, consistent with our remarks above.

The comparison to the Brookhaven-Columbia muon-pair experiment⁸ is shown in Figs. 7–10. The numerical calculations make no kinematic approximations, and should therefore correctly represent any phase-space threshold effect. The calculation also includes the effects of the experimental aperture (only μ pairs with laboratory longitudinal momentum greater than 12 GeV/c are considered). Figure 7 shows the experimental μ -pair mass distribution,⁸ and two theoretical curves, corresponding to the two extrapolations of the pion form factor shown in Fig. 11. In both cases, $F_{\pi}(Q^2)$ was taken from storage-ring data²⁴ on $e^+e^- \rightarrow \pi^+\pi^-$ for $Q^2 < 6$ GeV². For larger Q^2 , curve (a) represents a conventional extrapolation $F_{\pi}(Q^2) \sim 1.6/Q^2$, while curve (b) corresponds to an approximately constant cross section for $e^+e^- \rightarrow \pi^+\pi^-$ in the region 9 GeV² $< Q^2 < 25$ GeV². The latter behavior can be ruled out by data from SPEAR, since it would imply that $\sigma_{\pi^+\pi^-}/\sigma_{\mu^+\mu^-} \approx 2$ at $s = 25$ GeV².²⁵ All of our subsequent considerations are based on form (a) for F_{π} . If the recently discovered resonance at $m_{\mu\mu} = 3.1$ GeV (Ref. 15) is added to curve (a) as a

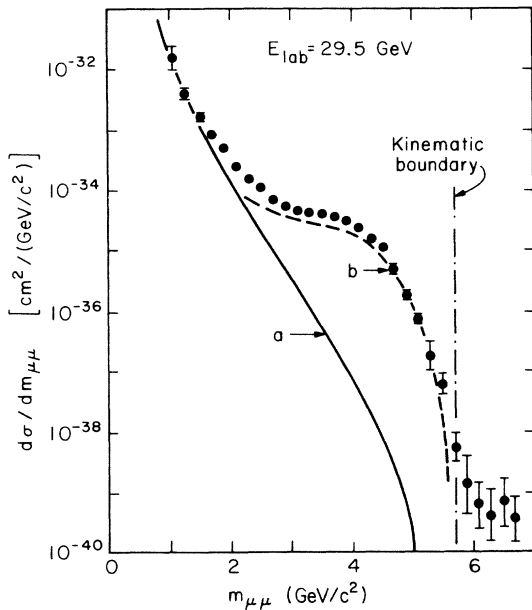


FIG. 7. Invariant mass distribution of the μ pair. The data are from Ref. 8. The two curves correspond to the two choices for F_{π} in Fig. 11.

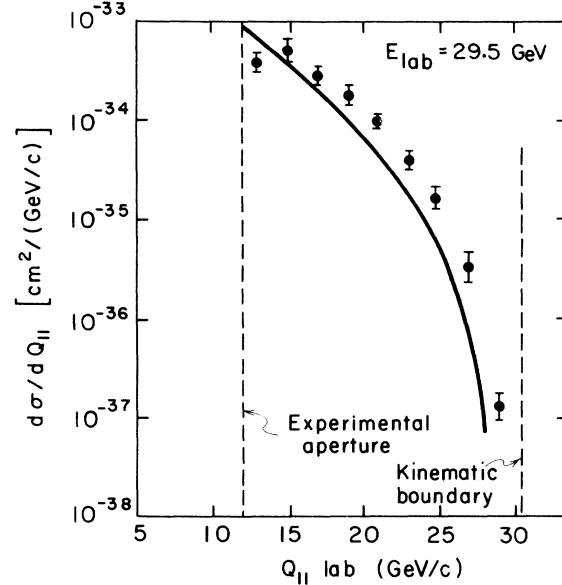


FIG. 8. Longitudinal momentum distribution in the lab frame of the μ pair. The data are from Ref. 8.

resolution-broadened bump, it is possible that the behavior of the distribution can be explained for the entire range in $m_{\mu\mu}$. Figures 8–10 show, respectively, the differential cross sections with respect to the longitudinal and transverse²⁶ components of virtual photon momenta and the total virtual photon cross section. The calculated

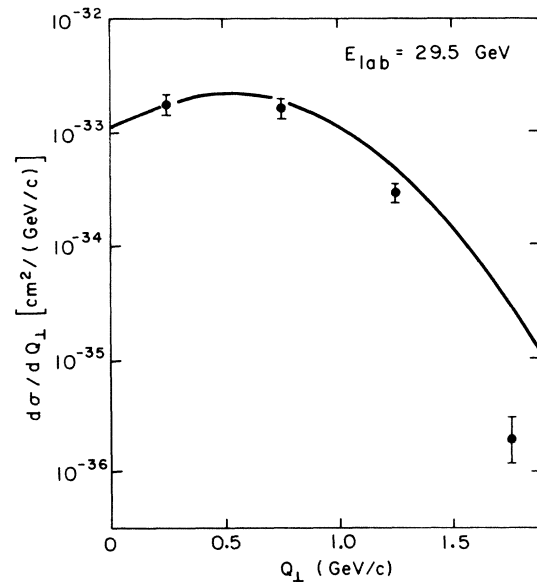


FIG. 9. Transverse momentum distribution of the μ pair. The data are from Ref. 8.

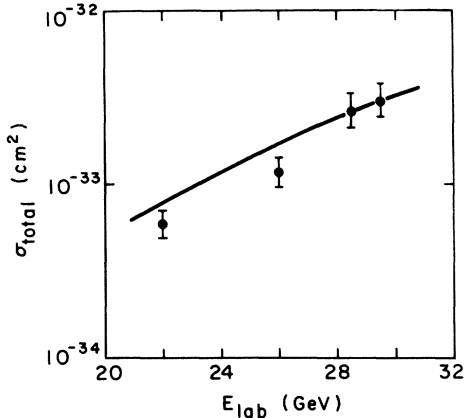


FIG. 10. Total μ -pair cross section. The data are from Ref. 8.

curves are in rough agreement with experiment, in most cases, except for the transverse momentum distribution at larger values of Q_{\perp} .

In Fig. 12 we compare the model with the single-muon transverse momentum distribution of the Chicago-Princeton experiment.⁹ The curve is generated using the choice (a) in Fig. 3 for the form factor. Most of the contribution to the cross section comes from events of low Q^2 , and our prediction is not sensitive to the presence of the new resonance at $m_{\mu\bar{\mu}} = 3.1$ GeV, at least for $p_{\perp} \lesssim 4$ GeV/ c . As in Fig. 9, the shape and normalization of the theoretical curve are consistent with experiment for smaller p_{\perp} ($p_{\perp} \lesssim 3$ GeV/ c), but the damping in the model seems too weak at larger values. It is worth noting that the quark-parton model predictions of Ref. 4 fall well below the data everywhere, and are almost two orders of magnitude too small at $p_{\perp} = 1.5$ GeV/ c . Experimentally, the ratio of the pion and muon inclusive cross sections is independent of the transverse momentum and approximately 10^4 . A multiperipheral model accounts for this ratio in a natural way, since the two production rates should be related by a roughly constant factor of order $1/\alpha^2$.²⁷

If indeed spin-0 exchange is responsible for μ -pair production, one may expect to observe a well-defined angular distribution for the muons in the pair rest frame. For example, if the exchanged pions are close to the mass shell, the distribution should be $\sin^2\theta$, where θ is the angle between one of the muons and one of the pions. Since there is a strong damping for off-mass-shell pions, and since the exchanged pions tend to be aligned along the beam axis, we expect that (at large Q^2) the distribution should be approximately $\sin^2\theta'$, where θ' is the Gottfried-Jackson angle. This is in contrast

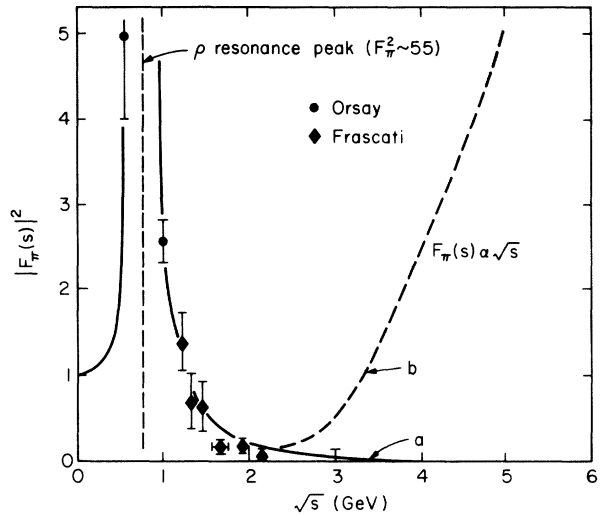


FIG. 11. Pion form factor. The data are from Ref. 24. The two curves correspond to those of Fig. 7. At large s , curve (a) represents the behavior $F_{\pi} \sim 1.6/s$.

to the parton-model expectation of a $1 + \cos^2\theta'$ distribution. Our assumption that pions are produced via ρ mesons means that the pion pairs are distributed like $\cos^2\theta'$. Thus, a model with spin-0 exchange must predict a muon transverse momentum distribution less damped than the pion. However, these effects may be washed out because the pion-like behavior we assume is just an average of multiperipheral production mechanism with (possibly) different angular distributions.

In Figs. 13–17, we present predictions for the

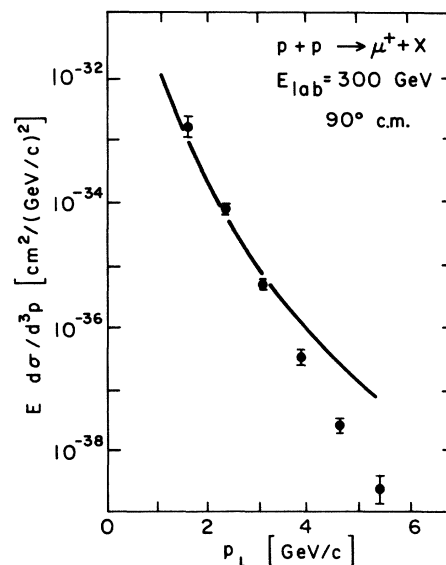


FIG. 12. Single-muon transverse momentum distribution. The data are from Ref. 9.

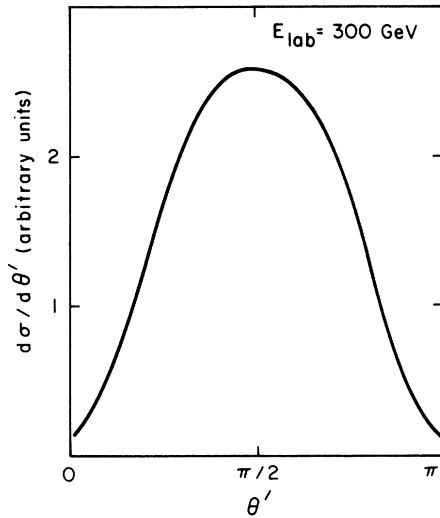


FIG. 13. Angular distribution of the muons. The Gottfried-Jackson angle θ' is the angle between the μ^+ and the proton beam measured in the μ -pair rest frame.

model which will be tested soon in experiments at Fermilab and the CERN ISR. With the qualifications of the preceding paragraph in mind, we show in Fig. 13 the expected angular distribution of the muons as a function of the Gottfried-Jackson angle, assuming pure pion exchange, at $E_{\text{lab}} = 300$ GeV. The curve includes muon pairs of all possible invariant masses.

Figure 14 shows the expected invariant mass dis-

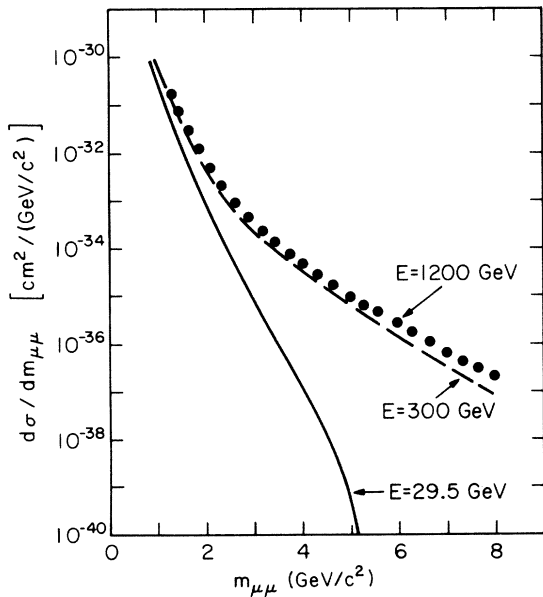


FIG. 14. Invariant mass distribution of the μ pair at high energies. The curves are generated with no limitations from the experimental aperture.

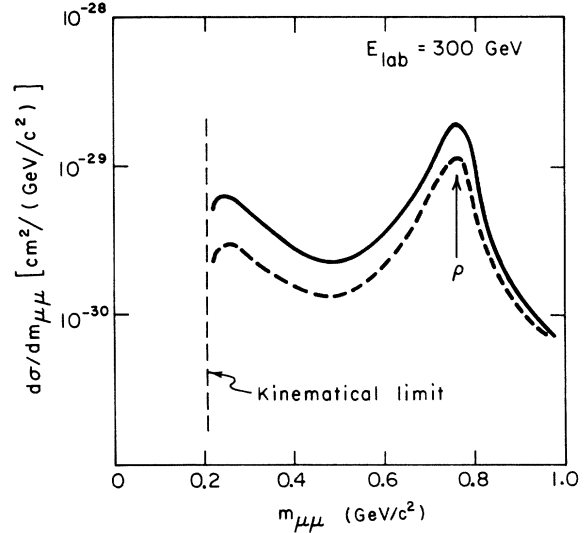


FIG. 15. Small invariant mass distribution of the μ pair. The dashed curve is the prediction with the experimental aperture Q_{\parallel} (in the lab) ≥ 12 GeV/c. The position of the ρ mass is indicated.

tributions at typical Brookhaven, Fermilab, and CERN ISR energies. The curves are generated without any aperture limitation on the longitudinal momentum of the muon pairs. The graph indicates that at $E_{\text{lab}} = 300$ GeV the invariant mass distribution has very nearly scaled, at least for $m_{\mu\mu} < 10$ GeV/ c^2 . The new resonances would appear as a sharp spike on top of our predicted curves.

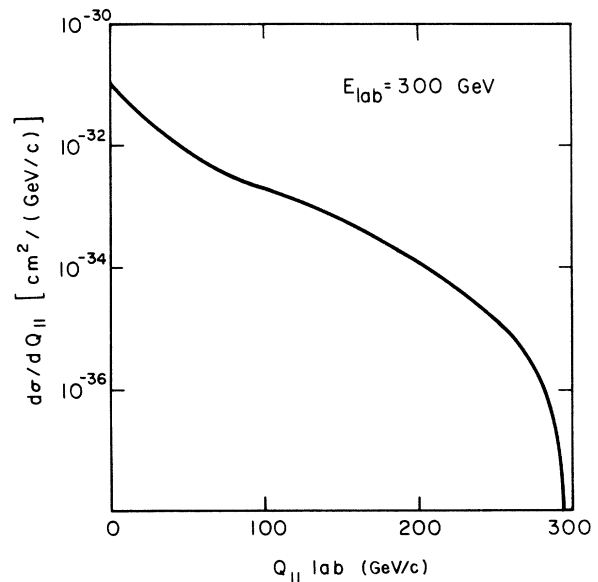


FIG. 16. Longitudinal momentum distribution of the μ pair in the laboratory.

Figure 15 shows the expected invariant mass distribution at $E_{\text{lab}} = 300$ GeV for small invariant mass. The dashed curve is the result with an experimental aperture limitation (Q_{\parallel} in the lab > 12 GeV/c). The ρ -meson peak is clearly visible as indicated.

Figures 16 and 17 show the expected distributions for Q_{\parallel} and Q_{\perp} of the muon pairs at $E_{\text{lab}} = 300$ GeV. The dashed curve in Fig. 17 is the result with the same aperture limitation (Q_{\parallel} in the lab > 12 GeV/c).

V. CONCLUSIONS

We conclude by suggesting that familiar hadronic processes may be responsible for most of the production of direct lepton pairs in hadronic collisions. The particular model we have studied is in rough agreement with all available data for values of transverse momentum and invariant mass that are not too large. Of course, at large invariant mass, the picture is clouded by the presence of the ψ and other new particles. Future experiments will test the model at higher energies and masses. In particular, it should soon be possible to choose between the different scaling laws expected from parton models and multiperipheral models.

ACKNOWLEDGMENTS

We are greatly indebted to many colleagues for discussions, comments, and criticism, particular-

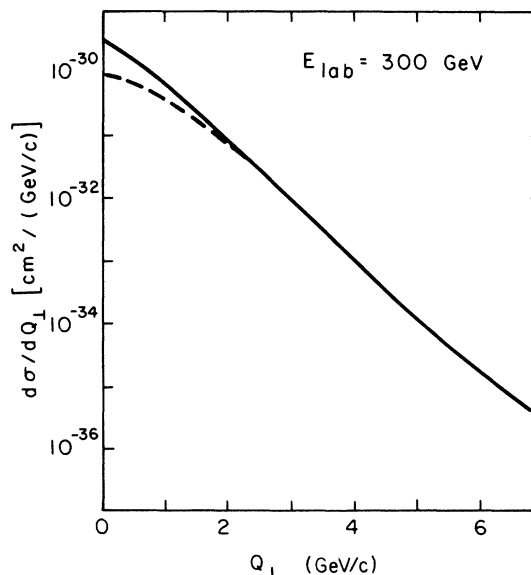


FIG. 17. Transverse momentum distribution of the μ pair. The dashed curve corresponds to Q_{\parallel} (in the lab) ≥ 12 GeV/c.

ly G. F. Chew, J. D. Jackson, A. H. Mueller, J. A. Shapiro, and M. Suzuki for helpful suggestions, and G. Goldhaber, B. Knapp, L. M. Lederman, W. Lee, F. Wagner, and F. Winkelmann for discussions of experimental questions.

*This research was supported by the U. S. Atomic Energy Commission.

¹S. D. Drell and T.-M. Yan, *Ann. Phys. (N.Y.)* **66**, 578 (1971).

²J. Kuti and V. F. Weisskopf, *Phys. Rev. D* **4**, 3418 (1971).

³P. Landshoff and J. C. Polkinghorne, *Nucl. Phys. B* **33**, 221 (1971).

⁴G. Chu and J. F. Gunion, *Phys. Rev. D* **10**, 3672 (1974).

⁵M. B. Einhorn and R. Savit, *Phys. Rev. Lett.* **33**, 392 (1974); *Phys. Rev. D* **10**, 2785 (1974).

⁶H. Parr and E. Paschos, *Phys. Rev. D* **10**, 1502 (1974).

⁷S. Pakvasa, D. Parashar, and S. F. Tuan, *Phys. Rev. D* **10**, 2124 (1974).

⁸J. H. Christenson *et al.*, *Phys. Rev. D* **8**, 2016 (1973).

⁹J. P. Boymond *et al.*, *Phys. Rev. Lett.* **33**, 112 (1974); similar results have been obtained by J. A. Appel *et al.* [*ibid.* **33**, 722 (1974)] and D. Bintinger *et al.* [presented at the spring, 1974 meeting of the American Physical Society, Washington, D.C. (unpublished)].

¹⁰L. Bertocchi, S. Fubini, and M. Tonin, *Nuovo Cimento* **25**, 626 (1962); D. Amati, S. Fubini, and A. Stanghellini, *ibid.* **26**, 896 (1962).

¹¹A brief account of this work appeared in G. Chu and J. Koplik, *Phys. Lett.* **55B**, 466 (1975).

¹²K. Subbarao, *Phys. Rev. D* **8**, 1498 (1973).

¹³H. B. Thacker, *Phys. Rev. D* **9**, 2567 (1973).

¹⁴D. Tow, *Phys. Rev. D* **2**, 154 (1970); G. F. Chew, T. Rogers, and D. R. Snider, *ibid.* **2**, 765 (1970).

¹⁵J. J. Aubert *et al.*, *Phys. Rev. Lett.* **33**, 1404 (1974);

J. E. Augustin *et al.*, *ibid.* **33**, 1406 (1974); C. Bacci *et al.*, *ibid.* **33**, 1408 (1974); G. S. Abrams *et al.*, *ibid.* **33**, 1453 (1974).

¹⁶Our normalization conventions are those of H. D. I. Abarbanel, G. F. Chew, M. L. Goldberger, and L. M. Saunders, *Ann. Phys. (N.Y.)* **73**, 156 (1972).

¹⁷A. Basetto, L. Sertorio, and M. Toller, *Nucl. Phys. B* **35**, 1 (1971).

¹⁸G. F. Chew and J. Koplik, *Nucl. Phys. B* **81**, 93 (1974).

¹⁹G. Giacomelli, in *Progress in Nuclear Physics*, edited by D. M. Brink and J. H. Mulvey (Pergamon, New York, 1969), Vol. 12, p. 77.

²⁰J. W. Cronin, *et al.* *Phys. Rev. Lett.* **31**, 1426 (1973).

²¹B. R. Webber, *Phys. Rev. Lett.* **27**, 448 (1971).

²²C.-I. Tan and D. M. Tow, *Phys. Lett.* **53B**, 452 (1975).

²³H. A. Gordon *et al.*, *Phys. Rev. Lett.* **34**, 284 (1975).

At low p_{\perp} , it is known that the number of produced pions is much larger than would result from ρ decay alone.

²⁴Data for $F_{\pi}(s)$ in the ρ region may be found in D. Be-

naksas *et al.*, Phys. Lett. 39B, 289 (1972) and V. E. Balakin *et al.*, *ibid.* 41B, 205 (1972). Data for larger values of s are given by V. Alles Borelli *et al.*, *ibid.* 40B, 433 (1972) and G. Barbiellini *et al.*, Nuovo Cimento Lett. 6, 557 (1973).

²⁵The data indicates $\sigma_{\pi^+\pi^-}/\sigma_{\mu^+\mu^-} \ll 1$; B. L. Beron *et al.*, Phys. Rev. Lett. 33, 663 (1974) and G. Goldhaber, private communication.

²⁶The unusually broad Q_{\perp} distribution is a kinematic effect resulting from the experimental aperture: Increasing Q_{\perp} at fixed (large) Q_{\parallel} lowers the virtual-photon ra-

pidity, and the decrease of the inclusive cross section with increasing Q_{\perp} is compensated by the excess of events at smaller rapidities. Pion inclusive spectra at these energies exhibit a similar behavior [P. Bosetti *et al.*, Nucl. Phys. B54, 141 (1973)], but the effect is weaker than for virtual photons because the latter are more massive and have a narrower rapidity distribution.

²⁷This effect has also been noted by R. M. Barnett and D. Silverman, Harvard report, 1974 (unpublished).